



## Insight of Photovoltaic Properties of (Diphenylamino) Pyren-1yl) Methylene) Malononitrile Compounds: DFT and TD-DFT Study

*Ikrame Nague<sup>a</sup>, Fatima-Ezaahra Loudifa<sup>a</sup>, Hajar Atmani<sup>a</sup>, Abderrahim Mouaddib<sup>a</sup>, Ahmed Jouaiti<sup>a</sup>*

<sup>a</sup> *Laboratory of Sustainable Development, Faculty of Sciences and Technologies, Sultan Moulay Slimane University, Beni Mellal, Morocco.*

### ABSTRACT:

In this research, an examination was operated on a series of molecules, namely 2-((7-(diphenylamino)pyren-1-yl)methylene)malononitrile, 2-((6-(diphenylamino)pyren-2yl)methylene)malononitrile, 2-((8-(diphenylamino)pyren-1-yl)methylene)malononitrile, and 2-((3-(diphenylamino)pyren-1-yl)methylene)malononitrile. The main focus was the investigation of their photovoltaic and electrical characteristics. Various parameters were determined through the application of theoretical calculations employing Density Functional Theory (DFT) and Time-Dependent DFT (TD-DFT) using alongside the B3LYP functional and the 6-31G basis sets. These measurements included the Molecular Electrostatic Potential (MEP), the Density Of States, the Partial Density Of States, the open-circuit voltage, and the evaluation of photovoltaic characteristics. The findings proved beyond a reasonable doubt that molecule 4 is the superior building block element, that promising prospects for improving the efficiency of high-performance organic solar cells.

**Keywords:** organic solar cells, photovoltaic properties, DFT/TD-DFT calculations, DOS and PDOS.

### Introduction:

Green energy such as solar energy has garnered significant attention in recent times due to its primary objective of reducing fossil fuel waste while swiftly meeting energy needs. The fast increase of the photovoltaic industry can be attributed to two factors: increasing demand for electricity and improvements in semiconductor technology[1]. Through photoemission phenomena, photovoltaic solar cells are able to transform the solar energy they absorb into electricity [2]. Energy conversion from photovoltaic solar cells depends on three criteria: donor, acceptor, and gap energies. Acceptor and donor are separated by a bridge or energy gap that lets electrons to flow from acceptor to donor, allowing acceptor to receive solar energy. There are three primary divisions of photovoltaic solar cells consist of: inorganic (made of semiconductor silicon materials), organic (made of polymers and micro-receptors), and hybrid (made of both organic and inorganic materials). [3]. Organic solar cells (OSCs) are distinguished from traditional silicon-based solar cells by several potential advantages, including large-area capabilities, flexibility, low cost, and ease of processing, but the silicon used in photovoltaics today is extremely expensive and hazardous to the environment[4].

Synthesizing and designing novel OSCs with narrow frequency bands has been a major area of research interest recently, and correlations have been discovered between molecule branching or donor group nature, performance characteristics, and photoelectric features [5][6]. Organic solar cells (OSCs) have two different types of materials in their active layers: An electron-donating (D) substance and an electron-accepting (A) substance [7]. The electron donor compounds have  $\pi$  electrons that can cause a transition  $\pi-\pi^*$  [8][9] By absorbing photons that are produced during the transition between the HOMO and LUMO orbitals. Pyrene-based molecules are very important compounds in many different fields. Due to their specific physical, chemical, and spectroscopic absorption and emission characteristics, they have found widespread use in solar cell and optoelectronics technologies. This is due to the fact that they spend a disproportionately large amount of time in an excited state with a high absorption rate. [9].

In this research, the theoretical methodologies DFT and TD-DFT with B3LYP and 6-31G basis sets have been used to obtain the subjective properties such as electronic and photoelectronic properties in order to show the practical application of these compounds in the field of photovoltaic cells. The four studied molecules are 2-((7-(diphenylamino)pyren-1-yl)methylene)malononitrile, 2-((6-(diphenylamino)pyren-2-yl)methylene)malononitrile, 2-((8-(diphenylamino)pyren-1-yl)methylene)malononitrile and 2-((3-(diphenylamino)pyren-1-yl)methylene)malononitrile named respectively mol1, mol2, mol3 and mol4.

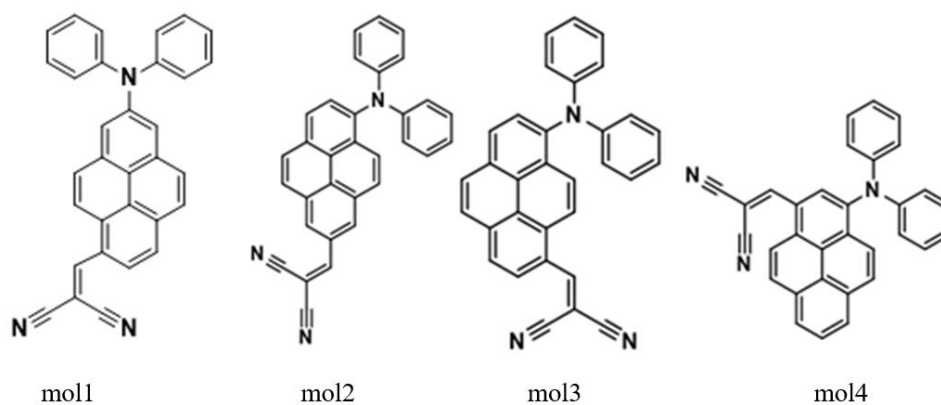


Figure 1 : studied compounds mol1, mol2, mol3 and mol4.

## 1. Computational Material :

The purpose of this research is to apply the Gaussian 09W software in order to extract information about electrical and spectroscopic properties of the studied molecules. [10]. The results were shown and the structures were drawn using the GaussView 6.0 software as well as to create and track UV absorption spectra of analyzed compounds [11]. Density functional theory (DFT) techniques were used to investigate the molecules geometries. The DFT/ B3LYP method with the 6-31G basis set was used to determine the energies HOMO, LUMO, and gap energies and to optimize the geometries of each molecule[12]. The density-time functional theory (TD-DFT) in conjunction with the B3LYP/6-31 G was used to determine electronic and photovoltaic characteristics for instance oscillator forces (f) and optical transitions[13]. Additionally, UV absorption spectra of the investigated compounds were generated and streaked using GaussView software[14]. The density of states (DOS) and Partial Density of States (PDOS) spectra were plotted using python.

## 2. Result and discussion :

### 2.1 Frontier molecular orbitals analysis :

An analytical analysis of the charge distribution on the frontier molecular orbitals (FMO) highest occupied molecular orbitals (HOMO) and lowest unoccupied molecular orbitals (LUMO) was used to investigate the electronic behavior of the examined compounds[15][16]. HOMO is thought to be the valence band and LUMO is the conduction band. The difference between the positions of the two bands are familiar as the HOMO-LUMO energy gap or band gap, the bonding and antibonding properties of the geometry of the molecule in the excited and ground states are explained by these parameters, and they have a significant impact on determining the photovoltaic characteristics of any energy device. which means that the HUMO and LUMO energy of organic molecules plays a key role in controlling and dictating the direction of charge transfer between the molecules' acceptors and donors.[17]. The FMO analysis was performed by DFT using GaussView software according the 6-31G energy level and the B3LYP technique. Table 1 represents finding of our study analyses and displays HOMO and LUMO orbital contour plots for the compounds under study.

Figure 2 depicts the optimal molecular shapes that were analyzed. The HOMO energy of the considered compounds has the following values: -5.3467, -5.2732, -5.3353, and -5.4256 eV. While the LUMO energy observed values as -2.9279, -2.8125, -2.9121, and -3.3151 eV for mol1, mol2, mol3, and mol4, respectively. Compared to mol1, mol2 and mol3, the mol4 molecule has a lower HOMO value (-5.4256 eV). An observation may be made regarding the substituted oligomers, wherein there is a gradual drop in the energy levels of the highest occupied molecular orbital (HOMO) and a corresponding increase in the energy levels of the lowest unoccupied molecular orbital (LUMO). This phenomenon results in a reduction of the band energy. [18]. When compared to mol1, mol3, and mol4, mol2 has higher HOMO values (-5.2732 eV). The low HOMO value of mol4 makes it more stable than any other chemical. (-3.3151 eV) is the LUMO energy level for a mol4 considering that the difference in energy levels between the HOMO and LUMO orbitals is 2.4188 eV for mol1, 2.4607 eV for mol2, 2.4231 eV for mol3, and 2.1105 eV for mol4, we can see that mol2 > mol3 > mol1 > mol4. The HOMO energies of the four compounds exhibit the characteristic aromatic nature, indicating electron delocalization across the entire conjugated molecule. It's noted that the LUMO energies of the compounds are centered on electron-deficient units on the right of the molecular chain. The energy gap is clearly extended from mol1 to mol2 when compared to the values of the gap energies for all these compounds. It is visible that these compounds with lowest energy gap are expected to have most exceptional photo-physical properties.

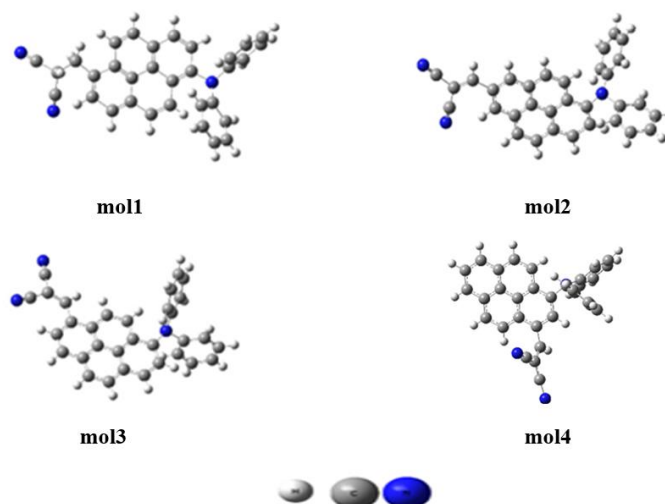
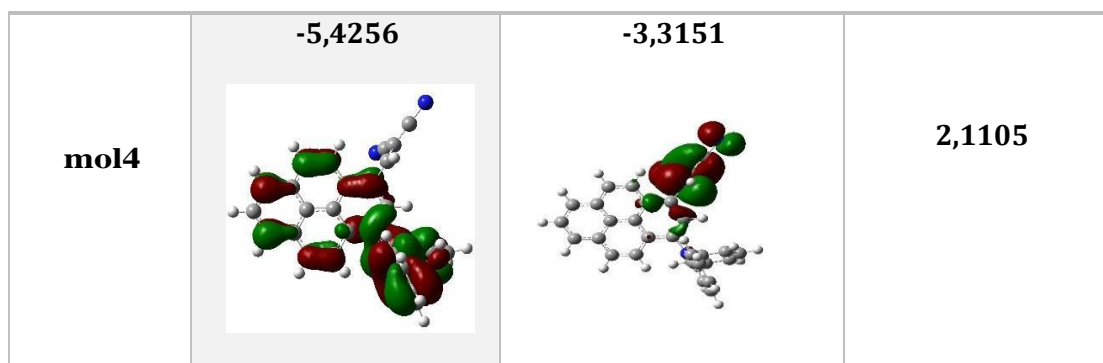


Figure 2 : The optimized geometrical structures of the studied molecules.

In order to evaluate the chance of electron transfer from the excited lowest unoccupied molecular orbital (LUMO) states of the compounds being examined into either the LUMO of the acceptor [6,6]-phenyl-C61-butyric acid methyl ester (PCBM) or the conduction band of titanium dioxide (TiO<sub>2</sub>), it will be essential to compare the LUMO levels of the compounds with the levels found in PCBM and the conduction band of TiO<sub>2</sub>. The LUMOs levels of all dyes are higher than that of PCBM (-3.2 eV)[19] and of the conduction band of semiconductor TiO<sub>2</sub> (-4.0 eV)[20]. This shows that these dyes are able to effectively inject electrons into the PCBM and TiO<sub>2</sub> acceptors.

**Tableau 1:** Energy of HOMO ( $E_{\text{HOMO}}$ ), energy of LUMO ( $E_{\text{LUMO}}$ ), energy gap ( $E_g$ ) and the contour plots of HOMO and LUMO orbitals of mol1, mol2, mol3 and mol4.

Mol	$E_{\text{HOMO}}$ (eV)	$E_{\text{LUMO}}$ (eV)	$E_g$ (eV)
mol1	-5,3467	-2,9279	2,4188
mol2	-5,2732	-2,8125	2,4607
mol3	-5,3353	-2,9121	2,4231



## 2.2 Open-circuit voltage :

The open circuit voltage ( $V_{oc}$ ) is used to approximate the efficiency of organic solar cells. It is directly correlated with the LUMO energy of the acceptor molecule and the HOMO energy of the donor one, this is calculated theoretically via the equation (1). It stands for the gap between the Highest Occupied Molecular Orbital (HOMO) energy levels of the studied compounds and the Lowest Unoccupied Molecular Orbital (LUMO) energy level of the electron acceptor [6.6]-phenyl-C61-butyric acid methyl ester (PCBM), or alternatively, relative to the conduction band of TiO<sub>2</sub>.

$$V_{oc} = |E_{HOMO}^{DONOR}| - |E_{LUMO}^{PCBM}| - 0.3 \quad \text{Equation (1)}$$

according to Table 2, the  $V_{oc}$  values of mol1, mol2, mol3 and mol4 are 1,3467 eV, 1,2732 eV, 1,3353 eV and 1,4256 eV for PCBM, and 1,0467 eV, 0,9732 eV, 1,0353 eV and 1,1256 eV for TiO<sub>2</sub> respectively. These outcomes hold significant implications for achieving a highly efficient electron injection into the LUMO states of either PCBM or TiO<sub>2</sub>.

Another measure  $\alpha_i$  was calculated by the difference between the LUMO energy levels of the investigated compounds and the LUMO energy level of PCBM.

$$\alpha_i = E_{LUMO}^{ACCEPTOR} - E_{LUMO}^{DONOR} \quad \text{Equation(2)}$$

As indicated in table 2, the  $\alpha_i$  values were in the range from 0.3849 eV to 0.8875 eV, which means that all LUMO level from all compounds is placed on LUMO level of PCBM.

**Table 2 :** Energy values of  $E_{HOMO}$ ,  $E_{LUMO}$  and  $V_{oc}$  for the studied compounds.

C	$E_{HOMO}(eV)$	$E_{LUMO}(eV)$	$V_{oc} (eV)$		$\alpha_i/ PCBM(eV)$
			PCBM	TiO <sub>2</sub>	
mol1	-5,3467	-2,9279	1,3467	1,0467	0.7721
mol2	-5,2732	-2,8125	1,2732	0,9732	0.8875
mol3	-5,3353	-2,9121	1,3353	1,0353	0.7879
mol4	-5,4256	-3,3151	1,4256	1,1256	0.3849
PCBM	-6,10	-3.7	-	-	-
TiO <sub>2</sub>		-4	-		

## 2.3 Photovoltaic properties :

Photovoltaic parameters include the molecule's excitation energy, oscillation strength, molecular orbital assignments, and absorption maxima [21]. Molecules with photovoltaic properties are evaluated for all compounds (mol1-mol4) using TD-DFT at the B3LYP/6-31G level.

The results of photovoltaic parameters are represented in Table 3 and simulated absorption maxima spectrum is depicted in Figure 2.

**Table 3:** absorption spectra values obtained with the TD/DFT method for the four compounds mol1, mol2, mol3, and mol4 in the optimized geometries at B3LYP/6-31G with  $E_{ex}$ : Excitation energy; f : Oscillator strength.

Electronic transitions		$\lambda_{abs} (nm)$	$E_{ex} (eV)$	f
mol1	S0 → S1	589.38	2.1036	0.3425
	S0 → S2	413.02	3.0019	0.4055
	S0 → S3	382.36	3.2426	0.2629
mol2	S0 → S1	595.23	2.0830	0.0089

mol3	S0 → S2	453.27	2.7353	0.2226
	S0 → S3	430.32	2.8812	0.0510
	S0 → S1	542.95	2.2835	0.2412
mol4	S0 → S2	457.62	2.7093	0.5592
	S0 → S3	382.60	3.2405	0.1362
	S0 → S1	779.45	1.5907	0.0047
	S0 → S2	643.54	1.9266	0.0248
	S0 → S3	475.59	2.6070	0.0012

The red-shifting of a molecule's absorption spectrum is generally reported to offer observed characteristics include a significant charge transfer, a noticeable absorption peak, and an impressive power conversion efficiency. The peak absorption values exhibited by mol. ( $\lambda_{\text{max}}$ :589.38 nm), mol2 ( $\lambda_{\text{max}}$ : 595.23 nm), mol3 ( $\lambda_{\text{max}}$ : 542.95 nm), and mol4 ( $\lambda_{\text{max}}$ : 779.45 nm) based on DFT observations. We discovered the following values for the force of the scout (f) for the same molecular order: 0.3425 , 0.0089 , 0.2412 , and 0.0047. The highest red-shifting in absorption spectra is reported for mol 4. The order of the studied compounds absorption maxima values are mol 4>mol 2>mol 1>mol 3. Since mol4 molecules showed strong red-shifting and good HOMO,LUMO assignments in comparison to the literature , it is obvious that mol4 is a good acceptor aspirant for high performance organic solar cells [22]. The excitation energy of organic solar cells is another useful metric to discover more their operation. At low excitation energies, excellent efficiency in power conversion and high charge transmission from the HOMO to LUMO levels are typically attainable [23][24]. The excitation energies of all molecules under study are determined by employing the B3LYP method with the 6-31G level of density-time functional theory. Excitation energy values of all compounds are 2.1036 eV (mol1), 2.0830 eV (mol2), 2.2835 eV (mol3), and 1.5907 eV (mol4). Among all compounds, mol 4 have the lowest excitation energy and the highest red-shifting and lowest HOMO-LUMO energy gap. As a result, the molecules 4 are useful building blocks for high-performance organic solar cells, as evidenced by their low excitation energy and significant red-shifting in the absorption spectrum.

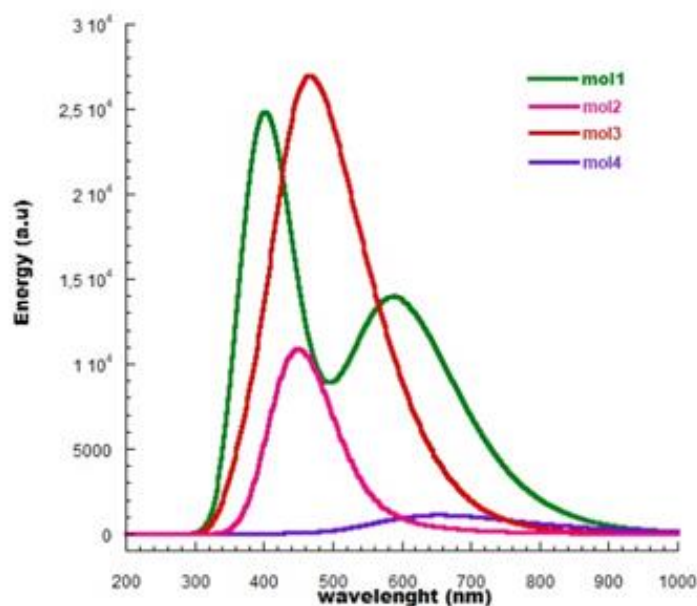


Figure 3 : The absorption spectra  $\lambda_{\text{max}}$  of the studied compounds.

#### 2.4 Density of states and partial density of states analysis:

Density of states (DOS) plots and partial density of states (PDOS) investigations are regarded as critical analyses for determining the performance of various acceptor molecules for organic solar cells. The electron density in the LUMO and HOMO associated with acceptor units of the examined compounds can be shown using DOS charts, and their distribution can be determined using PDOS plots.

The DOS and PDOS have been performed at B3LYP method along with 6-31G level for all studied molecules and the results obtained are depicted in figure 4. the energy gap and the distribution of states as functional of energy can be calculated using the density of states (DOS) method. In most cases, if the DOS value is high, many energy states are considered to be available while the zero value of DOS labels that there are no states accessible for energy level occupancy.

The most common application of density of states (DOS) is the conclusive factor in molecular orbital (MO) configurations. The DOS maps of the four compounds mol1-mol4 exploiting purple, blue, and black lines, illustrate the electronic distribution of the donor and acceptor bridge groups. (Fig4 )

shows the effect of the four proposed compounds' DOS plots of the bridge group on their distribution patterns, and also elucidate the orbital properties at various energy levels .

The HOMO and LUMO orbital energies beside the x-axis are respectively represented by the negative and positive energies, and the distance between positive and negative energies is shown by the HOMO-LUMO energy gap. It has been shown that the frontier molecular orbitals of the molecules mol1, mol2, mol3, and mol4 derive energy from the donor groups within the energy range of 20 to -10 eV.

The partial density of state (PDOS), which was assessed at the same functional level as DFT, provided further support to the conclusions obtained from frontier molecular orbitals (FMOs). It explains the states of the electrons in organic solar cells. HOMO density in all molecules is highly distributed on the donor part, moderately distributed on the core part, and rarely distributed on the acceptor part. And LUMO density is majorly present on end capped acceptor units in all compounds, with very little present on donor and core units. With the exception of molecule (mol4), almost all molecules displayed comparable distribution patterns of HOMO and LUMO electron density, probably because of structural resemblances. The distribution of HOMO density is present on the donor portion and extensive LUMO density on the acceptor part in the cases of mol 1, mol 2, and mol3. According to Fig. 4, The tailored acceptors were recognized as promising candidates for better solar cells by the PDOS study, which revealed significant delocalization, effective interaction between donor and acceptor regions, and dispersion of electron density.

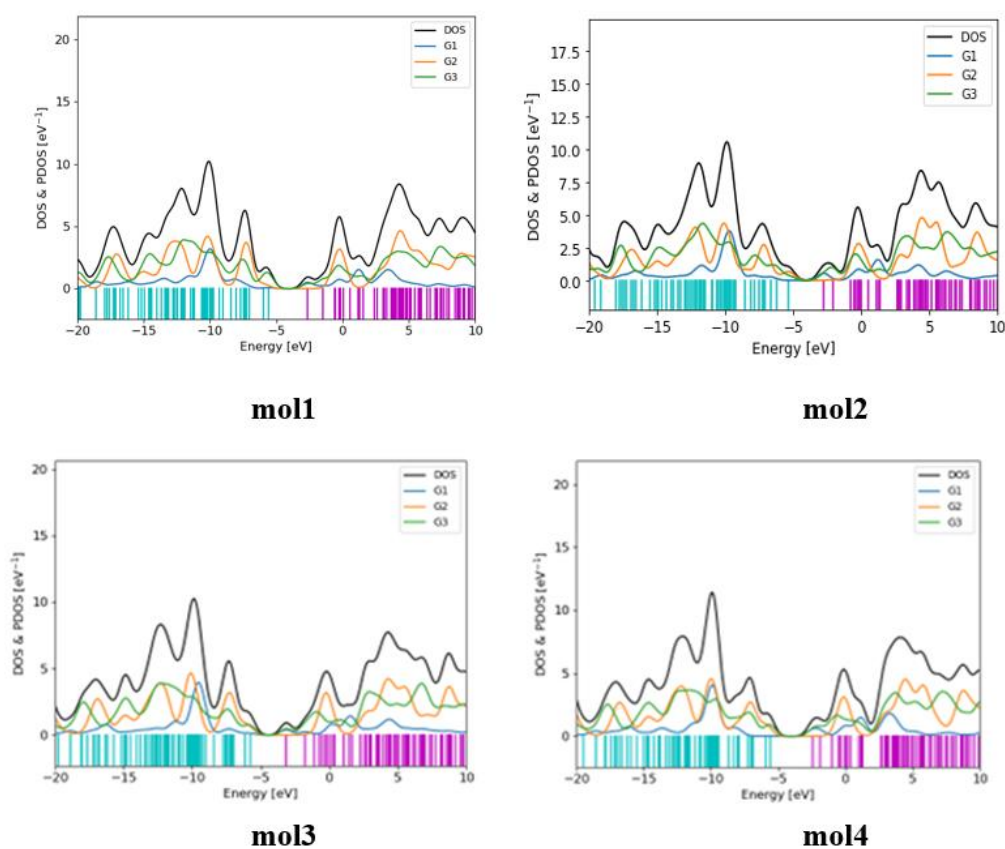


Figure 4 : DOS and PDOS plots off all studied molecules.

### 2.5 Molecular electrostatic potential (MEP) :

Molecular electrostatic potential (MEP) is used to analyze electrophile-nucleophile interactions and identify the reactive regions where hydrogen bonding interactions occur. The calculated MEP plots of all studied molecules (mol1 to mol4) have been shown in figure 5. The MEP plots provide several colored density cloud combinations on their map. Furthermore, the red parts depict the negative MEP while the blue parts reflect the positive MEP and the green parts indicate the neutral potential regions. The blue and red regions represent nucleophilic and electrophilic reactivity, respectively. It is noted that every compound has a significant charge separation. The results show that effective molecular design and modeling can create a highly efficient material for solar cell applications.

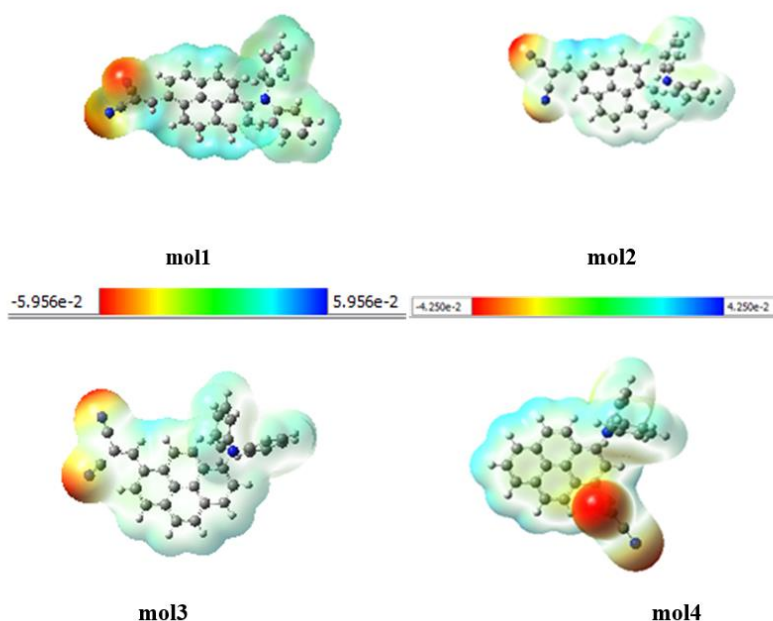


Figure 5 : MEP plots of all studied molecules (mol1-mol4) calculated with B3LYP/6-31G.

## Conclusion :

In the present paper, the theoretical analysis of the four organic molecules of 2-((N-(diphenylamino)pyren-1-yl)methylene)malononitrile has been carried out using the DFT and TD-DFT/B3LYP methods with the 6-31G basis set: mol1, mol2, mol3, mol4.

- Regarding the energies of the EHOMO and ELUMO, the computed band gap  $E_{gap}$  of the molecules under study ranged from 2,1105 eV to 2,4607 eV.
- The calculated  $V_{oc}$  values of the investigated compounds vary from 1.2732 eV to 1.4256 eV in the case of PCBM. Additionally, for TiO<sub>2</sub>, they vary from 0.9732 eV to 1.1256 eV.
- TD/DFT calculation were used to determine the UV-Vis absorption characteristics. Significant absorption maxima have been observed in the wavelength range of 542.95 nm to 779.45 nm.
- According to the DOS, MEP, and FMO maps, the generated molecules have in fact displayed good characteristics in terms of a decreased band gap and enhanced intermolecular charge transfer.

The computed theoretical is used to comprehend correlations between electrochemical characteristics and molecular structure. It may also be used to assume electronic properties of materials currently being developed and to create novel solar cell materials.

## References

- [1] D. Song, H. Jiao, and C. Te Fan, "Overview of the photovoltaic technology status and perspective in China," *Renew. Sustain. Energy Rev.*, vol. 48, pp. 848–856, 2015, doi: 10.1016/j.rser.2015.04.001.
- [2] M. Adnan, Z. Irshad, and J. K. Lee, "Facile all-dip-coating deposition of highly efficient (CH<sub>3</sub>)<sub>3</sub>NPbI<sub>3</sub>-: XCl<sub>x</sub>perovskite materials from aqueous non-halide lead precursor," *RSC Adv.*, vol. 10, no. 48, pp. 29010–29017, 2020, doi: 10.1039/d0ra06074g.
- [3] M. Naem, S. Jabeen, R. A. Khera, U. Mubashar, and J. Iqbal, "Tuning of optoelectronic properties of triphenylamines-based donor materials for organic solar cells," *J. Theor. Comput. Chem.*, vol. 18, no. 7, 2019, doi: 10.1142/S0219633619500366.
- [4] R. Friend, "Electroluminescence in conjugated polymers," p. CWE7, 2023, doi: 10.1364/cleo\_europe.1994.cwe7.
- [5] F. Huang et al., "Development of new conjugated polymers with donor- $\pi$ -bridge-acceptor side chains for high performance solar cells," *J. Am. Chem. Soc.*, vol. 131, no. 39, pp. 13886–13887, 2009, doi: 10.1021/ja9066139.
- [6] V. Jeux et al., "One step synthesis of D-A-D chromophores as active materials for organic solar cells by basic condensation," *Dye. Pigment.*, vol. 113, pp. 402–408, 2015, doi: 10.1016/j.dyepig.2014.09.012.
- [7] Y. Yi, V. Coropceanu, and J. L. Brédas, "Exciton-dissociation and charge-recombination processes in pentacene/C<sub>60</sub> solar cells: Theoretical insight into the impact of interface geometry," *J. Am. Chem. Soc.*, vol. 131, no. 43, pp. 15777–15783, 2009, doi: 10.1021/ja905975w.

- [8] L. Y. Zou, A. M. Ren, J. K. Feng, Y. L. Liu, X. Q. Ran, and C. C. Sunt, "Theoretical study on photophysical properties of multifunctional electroluminescent molecules with different  $\pi$ -conjugated bridges," *J. Phys. Chem. A*, vol. 112, no. 47, pp. 12172–12178, 2008, doi: 10.1021/jp8032462.
- [9] L. Siham, M. Bouchra, L. Latfa, and J. Ahmed, "Electronic and photoelectronic properties of N-(5-indazolyl)-arylsulfonamides molecules: DFT/TD-DFT study," 6th Int. Conf. Optim. Appl. ICOA 2020 - Proc., pp. 5–10, 2020, doi: 10.1109/ICOA49421.2020.9094521.
- [10] M. J. Frisch et al., "Gaussian 09, Revision B.01," Gaussian 09, Revis. B.01, Gaussian, Inc., Wallingford CT, pp. 1–20, 2009, [Online]. Available: citeulike-article-id:9096580
- [11] R. Suganda, E. Sutrisno, and I. W. Wardana, *GaussView 5 reference*, vol. 53, no. 9, 2013.
- [12] N. S. Babu, "DFT and TD-DFT studies of new triphenylamine-based (D-A-D) donor materials for high-efficiency organic solar cells," *Mater. Adv.*, pp. 3526–3535, 2022, doi: 10.1039/d2ma00048b.
- [13] P. W. Ayers, M. Levy, and Nagy, "Time-independent density functional theory for degenerate excited states of Coulomb systems," *Theor. Chem. Acc.*, vol. 137, no. 11, pp. 1–6, 2018, doi: 10.1007/s00214-018-2352-7.
- [14] Y. Lin, H. Fan, Y. Li, and X. Zhan, "Thiazole-based organic semiconductors for organic electronics," *Adv. Mater.*, vol. 24, no. 23, pp. 3087–3106, 2012, doi: 10.1002/adma.201200721.
- [15] S. Hussain et al., "Zinc-Doped Boron Phosphide Nanocluster as Efficient Sensor for SO<sub>2</sub>," *J. Chem.*, vol. 2020, 2020, doi: 10.1155/2020/2629596.
- [16] S. Hussain et al., "Adsorption of Phosgene Gas on Pristine and Copper-Decorated B12N12 Nanocages: A Comparative DFT Study," *ACS Omega*, vol. 5, no. 13, pp. 7641–7650, 2020, doi: 10.1021/acsomega.0c00507.
- [17] M. Ahmed et al., "Benzenesulfonohydrazides inhibiting urease: Design, synthesis, their in vitro and in silico studies," *J. Mol. Struct.*, vol. 1220, p. 128740, 2020, doi: 10.1016/j.molstruc.2020.128740.
- [18] P. F. De Athayde-Filho, J. Miller, A. M. Simas, B. F. Lira, J. A. De Souza Luis, and J. Zuckerman-Schpector, "Synthesis, characterization and crystallographic studies of three 2-aryl-3-methyl-4-aryl-1,3-thiazolium-5-thiolates," *Synthesis (Stuttg.)*, no. 5, pp. 685–690, 2003, doi: 10.1055/s-2003-38070.
- [19] M. Bourass et al., "DFT theoretical investigations of  $\pi$ -conjugated molecules based on thienopyrazine and different acceptor moieties for organic photovoltaic cells," *J. Saudi Chem. Soc.*, vol. 20, pp. S415–S425, 2016, doi: 10.1016/j.jscs.2013.01.003.
- [20] E. Van Loon and L. Stroosnijder, "Evidences of hot excited state electron injection from sensitizer molecules to TiO<sub>2</sub> nanocrystalline thin films," *Res. Chem. Intermed.*, vol. 27, no. 4–5, pp. 393–406, 2001, doi: 10.1163/156856701104202255.
- [21] M. Y. Mehboob, M. Adnan, R. Hussain, and Z. Irshad, "Quantum chemical designing of banana-shaped acceptor materials with outstanding photovoltaic properties for high-performance non-fullerene organic solar cells," *Synth. Met.*, vol. 277, no. January, p. 116800, 2021, doi: 10.1016/j.synthmet.2021.116800.
- [22] M. U. Khan et al., "Designing triazatruxene-based donor materials with promising photovoltaic parameters for organic solar cells," *RSC Adv.*, vol. 9, no. 45, pp. 26402–26418, 2019, doi: 10.1039/c9ra03856f.
- [23] S. Hussain et al., "Designing Novel Zn-Decorated Inorganic B12P12Nanoclusters with Promising Electronic Properties: A Step Forward toward Efficient CO<sub>2</sub>Sensing Materials," *ACS Omega*, vol. 5, no. 25, pp. 15547–15556, 2020, doi: 10.1021/acsomega.0c01686.
- [24] S. A. Siddique et al., "Efficient tuning of triphenylamine-based donor materials for high-efficiency organic solar cells," *Comput. Theor. Chem.*, vol. 1191, no. October, p. 113045, 2020, doi: 10.1016/j.comptc.2020.113045.